Postprint of: Marczyński R., Szostak J., Signerski R., Jarosz G.: *Photovoltaic effect in the single-junction DBP/PTCBI organic system under low intensity of monochromatic light*, Current Applied Physics 19 (2019) 1271–1275, DOI: 10.1016/j.cap.2019.08.011

# Photovoltaic effect in the single-junction DBP/PTCBI organic system under low intensity of monochromatic light

Rafał Marczyński, Justyna Szostak, Ryszard Signerski, Grażyna Jarosz*
*Faculty of Applied Physics and Mathematics*, Gdansk University of Technology, G. Narutowicza 11/12, 80-233 Gdańsk, Poland

**Abstract**

Photoelectric properties of the planar ITO/$MoO_3$/DBP/PTCBI/BCP/Ag system were characterized on the basis of short-circuit current, open-circuit voltage and absorption spectra, and current-voltage measurements in the dark and under monochromatic illumination of low intensity. Photovoltaic performance of the system was compared with the performance of ideal semiconductor and excitonic cells of chosen bandgaps. Such analysis shows, that the fabricated cell exhibits quite high value of the open-circuit voltage, in comparison to the SQ limits calculated for semiconductor devices of bandgaps close to the $LUMO_{PTCBI}$-$HOMO_{DBP}$ offset or crystalline silicon cells of the same absorptivity. This confirms that the DBP/PTCBI junction exhibits good properties for conversion of exciton energy to chemical energy of electron-hole pair. Moreover, open-circuit voltage and short-circuit current of the investigated cell practically do not change within the *520* nm–*620* nm range, for which they reach the maximum values, making the junction of DBP/PTCBI attractive for use in indoor photovoltaics.

*Keywords:* Organic photovoltaic cell, Planar heterojunction, Shockley-Queisser limit, Charge transport, Excitonic photovoltaic cell

## Introduction

One of the main processes determining the effectiveness of energy conversion in organic photovoltaic cells is the exciton dissociation, that takes place mainly at the electron donor (D)/electron acceptor (A) interface. The rate of this process is affected by many factors, among which the energetic structure of the layers forming the D/A junction, as well as, the exciton flux reaching this junction play major roles. Hence, it is vital for the performance of the cell to enhance the number of excitons generated in the vicinity of the D/A interface. One of the possible ways leading to such an enhancement is to choose highly absorptive materials keeping the thickness of the top illuminated organic layer limited to a value not much larger than the exciton diffusion length in this material. Moreover, if strong absorption of the bottom layer does not coincide with the efficient absorption of the top film, both of the active materials may simultaneously contribute to light harvesting and photocurrent generation. Unfortunately, due to finite widths of absorption bands of organic solids, the total absorptivity of a single junction organic system is always lower than the absorptivity of its inorganic semiconductor p-n counterpart. This is one of the reasons why the efficiency of organic single junction solar cells (SJOSCs), peaking *11.2%* at the moment, is much lower than the *28.8%* effectiveness [1], almost equal to the Shockley-Queisser (SQ) limit [2], reached by respective inorganic systems. What is the limit of the energy conversion efficiency of SJOSCs still remains an open question. Despite the undoubted superiority of classical semiconducting p-n junction solar cells described above, it has been suggested that organic devices could successfully compete with the inorganic ones in some special applications, such as indoor photovoltaic cells working under artificial illumination [3], i.e. illumination of intensity lower than solar illumination and limited to a relatively narrow spectral range. In such applications very strong absorption of light in a proper range of wavelengths, e.g. *450–650* nm in the case of illumination provided by white LEDs [4], along with simple and cheap fabrication methods, low weight, flexibility and semitransparency of organic photovoltaic devices would be a real benefit. These cells could be used to power small electronic devices and sensors, extend the lifespan of batteries, or serve the role of light detectors sensitive to illumination intensity.

Herein we present the results of the study carried out for a single electron donor/electron acceptor heterojunction system that could be applied as an indoor photovoltaic cell. We analyze the short-circuit current ($J_{sc}$) and open-circuit voltage ($V_{oc}$) action spectra of the device with respect to the absorption spectra of both organic active materials. We compare the photovoltaic performance of the fabricated cell recorded under monochromatic illumination of low intensity, and the wavelength corresponding to the maximum value of $J_{sc}$,

with the photovoltaic performance of theoretical, most efficient single junction semiconductor cells of chosen bandgaps and excitonic cells, working under identical illumination conditions. Photovoltaic parameters of these cells are calculated within the frame of the modified SQ model [2,5]. The purpose of such a comparison, that is a common practice for photovoltaic devices [6–9], is to determine the utility of the investigated system via assessment of the obtained values of photovoltaic parameters of our device with respect to the hypothetical maximum ones, possible to achieve for a single junction semiconductor photovoltaic cell.

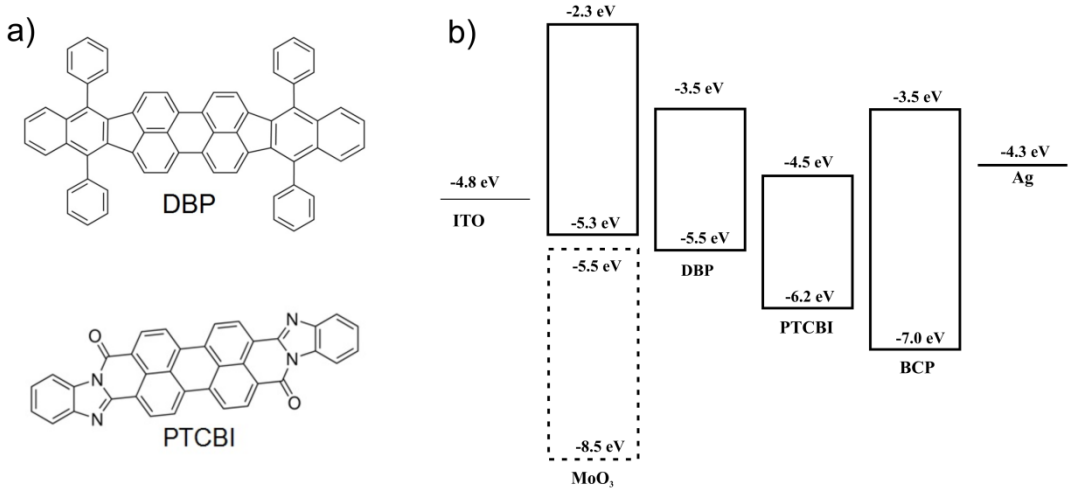


**Fig. 1.** Chemical structure of organic active materials, i.e. DBP and PTCBI, (a), and the energetic structure of layers of all the materials forming the investigated devices, i.e. ITO [10–12], $MoO_3$ [13–15], DBP [10,13], PTCBI [16,17], BCP [10,13,17], and Ag [18] (b).

The system of interest was based on a fullerene-free planar heterojunction formed by two perylene dyes, namely PTCBI (perylenetetracarboxylic bisbenzimidazole) and DBP (tetraphenyldibenzoperiflanthene) of chemical structures shown in Fig. 1a. The former compound, a well-known organic dye utilized by Tang [19], was used as an electron acceptor [17], while the latter material, forming homogeneous layers of high linear coefficients of absorption of light, exceeding $4 \cdot 10^5$ $cm^{-1}$, when deposited by means of thermal evaporation [10,13,20], was employed as an electron donor [10,13,20–23]. These properties, along with the facts, that i) relative positions of *HOMO* and *LUMO* levels in DBP and PTCBI (see Fig. 1b) seem to provide suitable conditions for efficient exciton dissociation, and for high values of the open-circuit voltage approaching *1.0* eV, ii) high values of $V_{oc}$ were already reported for some heterojunction solar cells utilizing DBP as an electron donor, iii) in contrast to fullerene solar cells [24–26], devices with perylene dyes show quite high thermal and air stability [27–30], iv) both active materials show pronounced absorption of light in the *500–650* nm spectral range, characteristic for artificial illumination and sunlight, account for such a choice of the active materials. It is worth mentioning, that uncertainties of HOMO levels determined from the UPS measurements are equal to *0.1-0.2* eV, while uncertainties of LUMO positions are greater, and reach *0.3-0.5* eV for the IPES technique [31]. To the best of our knowledge, there are no studies concerning the photovoltaic performance of a cell based on the planar DBP/PTCBI heterojunction, and the only report regarding a solar cell employing this set of active materials concerns a bulk DBP:PTCBI heterojunction of low concentration of DBP, showing low value of $V_{oc}$ and poor performance under AM 1.5 G illumination [32].

## Experimental

Thin layers of $MoO_x$ (*5* nm), DBP (*38* nm), PTCBI (*60* nm), bathocuproine (BCP, *15* nm) and Ag (*60* nm) were subsequently deposited via thermal evaporation under high vacuum of $5 \cdot 10^{-6}$ hPa on clean glass substrates partially cover by ITO. Deposition rate did not exceed *0.5* Å/s. $MoO_x$ with $x < 3$, that is formed due to oxygen loss occurring during thermal evaporation of $MoO_3$, was incorporated into the system to facilitate hole extraction from DBP to ITO, as well as to reduce exciton quenching at ITO [20,33–37], while BCP was used to improve electron collection at Ag electrode, and to prevent damage of the acceptor layer caused by penetration of this layer by Ag atoms upon their deposition [20,21,33–35]. As a result, ITO/$MoO_x$/DBP/PTCBI/BCP/Ag cells of the active area equal to *4* $mm^2$ were fabricated. The energetic structure of this system with two alternative views on the band diagram of $MoO_3$ [13,15] was shown in Fig. 1b. All measurements were carried out in ambient air without encapsulation. The thickness of each layer was estimated on the basis of microbalance measurements. In

addition, the thicknesses of DBP and PTCBI layers were confirmed by the comparison of the measured absorbance spectra to the ones reported in literature.

**Results and discussion**

Fig. 2 shows short-circuit current and open-circuit voltage action spectra, recorded for the investigated cell illuminated through ITO with a constant photon flux of $I_0 = 10^{14}$ $cm^{-2}s^{-1}$ at the ITO/$MoO_x$ interface, with respect to the absorption spectra of single layers of DBP and PTCBI, fabricated in the same cycle as the cell. Since these action spectra correspond well with the absorption spectra of both active layers, and short-circuit current flows in the sample from Ag to ITO, we may imply that free charge carriers originate from exciton dissociation taking place at the DBP/PTCBI interface. Holes are transported through DBP to ITO, while electrons flow towards the Ag electrode via PTCBI. It is seen that under such illumination conditions excitons photogenerated in both active materials contribute to photocurrent and photovoltage. For the wavelengths greater than *650* nm both of these physical quantities are determined by dissociation of excitons generated in PTCBI, as the absorption of DBP in this range is relatively weak, while $J_{sc}$ and $V_{oc}$ action spectra follow the absorption spectrum of the acceptor layer. One of the factors accounting for the fact, that values of $J_{sc}$ and $V_{oc}$ in this range are relatively low might be the short exciton diffusion length in this material [17,38,39] (see Table 1). In the range of strong absorption of light by DBP and PTCBI, i.e. from ca. *450* nm to ca. *650* nm, $V_{oc}$ and $J_{sc}$ action spectra correspond well with the absorption spectrum of the investigated system (see the inset in Fig. 2), while the absorbance of $MoO_x$ and BCP layers for $\lambda > 400$ nm is practically negligible. Minor shifts between the absorption and $J_{sc}$ and $V_{oc}$ peaks may be related to the overall effect of filtering of light by DBP, and changes in the contribution of excitons generated in DBP and PTCBI to photocurrent.

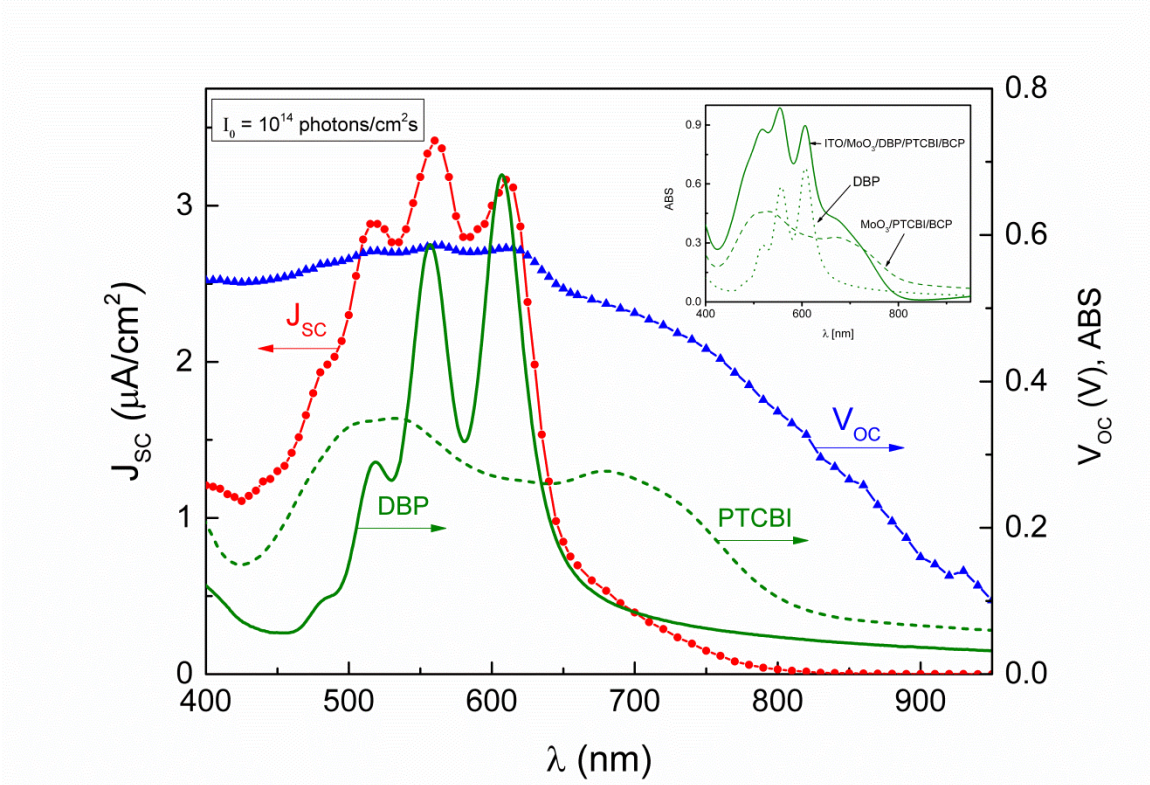


**Fig. 2.** Short-circuit current (circles) and open-circuit voltage (triangles) action spectra of the ITO/$MoO_x$/DBP/PTCBI/BCP/Ag cell illuminated through ITO at a constant photon flux of $I_0 = 10^{14}$ $cm^{-2}s^{-1}$ at the ITO/$MoO_x$ interface, and absorbance (ABS) of DBP (solid line) and PTCBI (dashed line). Inset: Absorbance of DBP (dotted), $MoO_3$/PTCBI/BCP (dashed), and ITO/$MoO_3$/DBP/ PTCBI/BCP (solid) systems.

**Table 1.** Exciton diffusion lengths in the investigated active layers.

| Material | Diffusion length |
|---|---|
| DBP | 16 nm [13] or 7 nm [22] |
| PTCBI | 3-5 nm [17,38,39] |

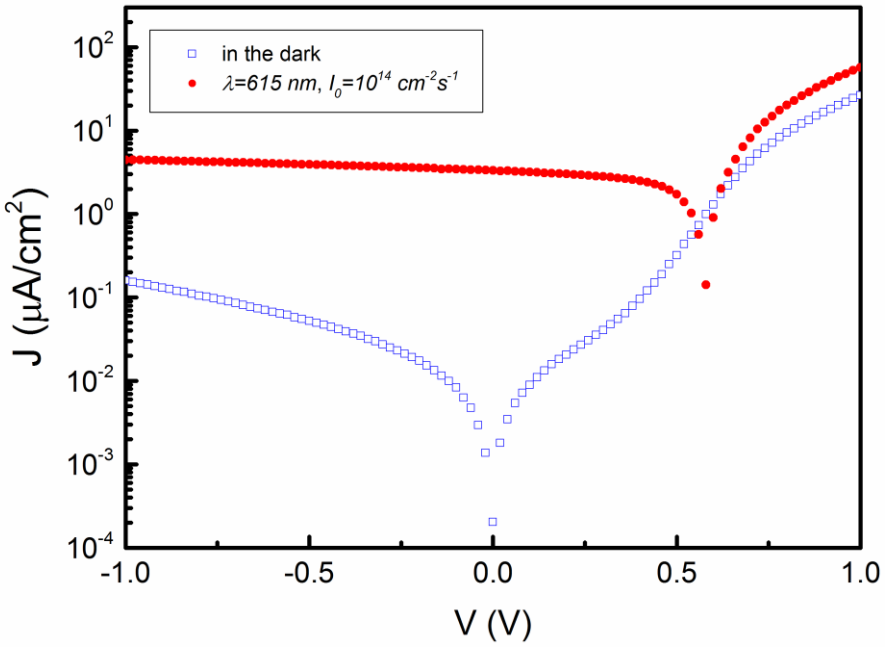


**Fig. 3.** Current-voltage curves collected in the dark (squares), and under monochromatic illumination through ITO of intensity $I_0 = 10^{14}$ cm$^{-2}$s$^{-1}$ and wavelength $\lambda_o = 615$ nm (circles).

Fig. 3 shows current-voltage curves collected in the dark, and under monochromatic illumination of intensity $I_0 = 10^{14}$ cm$^{-2}$s$^{-1}$, and wavelength $\lambda_o = 615$ nm corresponding to the peak of the short-circuit current action spectrum in the absorption band of DBP (see Fig. 2). Rectifying behavior is clearly seen for the dark curve, but reverse current is nonlinearly dependent on the applied voltage, and its saturation is not observed even under relatively high bias. Moreover, two very short exponential parts of this curve can be distinguished for the forward bias, indicating that the Shockley equation does not seem to be applicable for the investigated system, which is quite common for organic solar cells [10,40,41]. Short-circuit current density, open-circuit voltage, fill factor, and energy conversion efficiency obtained under monochromatic illumination described above, were equal to *3.32* μA/cm², *0.58* V, *0.52* and *3*%, respectively. The latter was calculated as the ratio of the maximum power generated by the photovoltaic cell to the power of the incident illumination, and it does not seem to be impressive when compared to the values of efficiency of the best single-junction organic solar cells. Our device, however, is free of fullerene and stable in the air. Non-fullerene organic solar cells have attracted much attention in recent years due to their rapidly increasing power conversion efficiency [42,43]. Nevertheless, a simple comparison between the performance of our cell and solar cell is not very informative if we consider a cell for indoor application. To assess the potential efficiency of such a system we may calculate the SQ limit for an ideal single-junction device under regarded illumination conditions. For this purpose, we will now assume that the bandgap of hypothetical ideal system is equal to the $LUMO_{acceptor}$-$HOMO_{donor}$ offset, namely $E_{g1} = 1.0$ eV in the case of DBP and PTCBI, that is believed to determine the maximum value of the open-circuit voltage in organic solar cells [44,45]. We will also compare the performance of our cell with the SQ limit obtained for the $E_{g2} = 1.1$ eV, which is a bandgap of crystalline silicon. So far it is the material most often used for photovoltaic applications. We shall assume that the absorptivity of a the system, which is a function of photon energy ($\hbar\omega$), is equal to 0 for photons of energy lower than the bandgap, and to *0.86* for photons of energy greater equal than the bandgap. The value of *0.86* was chosen, since according to the following formula

$$a = 1 - 10^{-(ABS_{DBP} + ABS_{PTCBI})} \quad (1)$$

this is the absorptivity of our system measured at $\lambda_0 = 615$ nm, where $ABS_{DBP}$ and $ABS_{PTCBI}$ stand for the absorbance of DBP and PTCBI, respectively. Furthermore, only radiative recombination is taken into account, and the temperature of the cell $T_C$ is equal to *293* K. In the SQ model current $J_{SQ}$ flowing through a biased cell, illuminated with light of wavelength $\lambda_0$ and intensity $I_0$ is equal to [2,5]:

$$J_{SQ} = J_0 \left[ exp\left(\frac{eV}{kT_c}\right) - 1 \right] - J_G \tag{2}$$

with

$$\frac{J_0}{e} = \frac{1}{2\pi^2 \hbar^3 c^2} \int_0^{+\infty} \frac{a*(\hbar\omega)^2}{exp\left(\frac{\hbar\omega}{kT_c}\right)-1} d(\hbar\omega) \tag{3}$$

and

$$J_G = e a_o I_o \tag{4}$$

where $J_o/e$ stands for the effective number of radiative recombination acts per unit of time and unit area of an unbiased cell, that follows from the principle of detailed balance, regarding electromagnetic radiation absorbed and emitted by a flat solar cell surrounded by a blackbody at temperature $T_C$, while $J_G$ is a generation current resulting from illumination of the cell. *V, e, k, $a_0$, ħ*, and *c* refer to the applied bias, elementary charge, Boltzmann constant, absorptivity of the material for the wavelength $\lambda_0$, Planck constant divided by $2\pi$, and speed of light in free space, respectively.

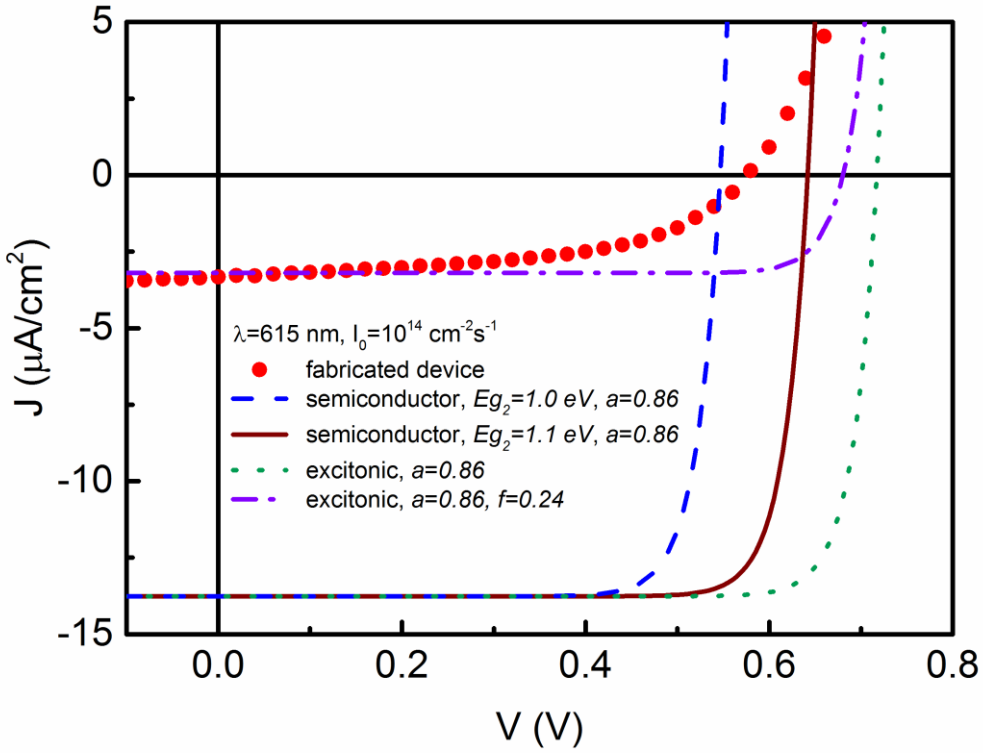


**Fig. 4.** Theoretical current-voltage curves, resulting from the modified SQ model (Eqs. (1) and (2)) for ideal single-junction semiconductor cells of $E_{g1} = 1.0$ eV (dashed blue) and $E_{g2} = 1.1$ eV (solid brown) at absorptivity $a = 0.86$ for photons of energy $E_f > E_g$; theoretical current-voltage curves, resulting from the modified SQ model applied to excitonic solar cells of absorptivity of *0, $10^{-3}$*, and *0.86* for the photons of energy $E_f < 1.0$ eV, *1.7* eV ≥ $E_f \geq 1.0$ eV and $E_f > 1.7$ eV, respectively, and at $f = 0.86$ (dotted green) and $f = 0.24$ (dashed-dotted violet), along with the experimental J-V characteristics (red circles) collected for the investigated cell under the same illumination conditions, i.e. under monochromatic illumination of $\lambda_0 = 615$ nm and photon flux $I_0 = 10^{14}$ cm$^{-2}$s$^{-1}$.

Theoretical current-voltage curves, resulting from this modified SQ model (Eqs. (2)–(4)) for $E_{g1} = 1.0$ eV and $E_{g2} = 1.1$ eV (blue dash and wine solid lines), along with the experimental J-V characteristics (red circles) collected for the investigated cell under the same illumination conditions, i.e. under monochromatic illumination of $\lambda_0 = 615$ nm and photon flux $I_0 = 10^{14}$ cm$^{-2}$s$^{-1}$, are shown in Fig. 4, while calculated and measured values of $J_{sc}$ and $V_{oc}$ are presented in Table 2. *J-V* characteristics of all real single-junction semiconductor devices of the same bandgap and the same absorptivity, but subject to additional non-radiative losses, should lie within the area enclosed by the respective $J_{SQ}$ curves and voltage axis. Interestingly, our cell shows a relatively high value of the open-circuit voltage, that is only 60 mV lower than the maximum $V_{oc}$ predicted by the SQ limit for the silicon bandgap, and higher than the maximum value predicted for the semiconductor system with a bandgap of *1.0* eV

under these illumination conditions. Thus, our experimental $V_{oc}$ exceeds the SQ limit for the bandgap equal to the $LUMO_{acceptor}$ - $HOMO_{donor}$ difference. This fact can be explained when the differences in absorptivity of excitonic and inorganic semiconductor materials are taken into account. Firstly, it is worth noticing that in the case of ideal semiconductor systems radiative recombination, following from high absorptivity of photons of energy greater than the bandgap and the principle of detailed balance between the absorbed and emitted radiation, is a major factor limiting $V_{oc}$. Moreover, it is well known, that the absorptivity of organic cells is much lower than *1* for the photons of energy greater equal to the $LUMO_{acceptor}$ – $HOMO_{donor}$ offset and lower than the bandgap. Giebink et al. claim that in this range of wavelengths this parameter can be as low as $10^{-3}$ [46], while Seki et al. suggest that it can be even equal to zero [47]. Low value of absorptivity of our cell in this spectral range may account for the fact, that experimental value of $V_{oc}$ exceeds the theoretical limit calculated above, confirming that the limit SQ is rather not applicable to organic devices. Giebink et al. and Seki et al. have proposed a modified SQ model for excitonic cells taking into account the fact, that in the case of these cells absorption of light leads to creation of bound electron-hole pairs of high exciton binding energies of around *0.3-0.5* eV. Photogeneration of strongly bound electron-hole pairs is the reason why the efficiency of energy conversion of organic cells, will always be lower than the efficacy of inorganic cells of the same bandgap under solar radiation [44–47]. These excited states can effectively dissociate only in the vicinity of the D/A interface of suitable $HOMO_{donor}$ - $HOMO_{acceptor}$ and $LUMO_{donor}$ - $LUMO_{acceptor}$ offsets, for which interface CT excitons, with holes localized on donor molecules and electrons located at the adjacent acceptor molecules, are created. The main determinant of the energy of an interface CT pair is the $LUMO_{acceptor}$ - $HOMO_{donor}$ difference, that according to literature is equal to about *1.0* eV for the DBP/PTCBI heterojunction. Since the energy bandgaps of DBP and PTCBI are equal to about *2.0* eV and *1.7* eV, respectively, we shall consider two different energetic gaps to estimate the limit of $V_{oc}$ for the regarded excitonic cell, namely the energy band gap of the organic semiconductor equal to *1.7* eV and the energy of the interfacial CT state equal to *1.0* eV, and assume that the absorptivity of the system in question is equal to *0, $10^{-3}$* (after Giebink et al. [46]), and *0.86* for the photons of energy $E_f$ < *1.0* eV, *1.7* eV ≥$E_f$ ≥ *1.0* eV , and $E_f$ > *1.7* eV, respectively. Under these assumptions we would obtain the maximum $V_{oc}$ of *0.715* V (see the dotted line $J_{ex}$ in Fig. 4), which is only *0.135* V greater than the experimental value of this parameter, and, what is important, greater than the maximum $V_{oc}$ calculated for an ideal semiconductor device of $E_{g1}$=*1.0* eV. The experimental value of $V_{oc}$ recorded for our sample reaches *80*% of the maximum value calculated from the SQ model adapted for excitonic cells. Such a comparison does not let us identify the processes responsible for the observed energetic losses, but it confirms that the energy of the electron-hole pair generated at the DBP/PTCBI interface as a result of exciton dissociation is determined by the $LUMO_{acceptor}$ - $HOMO_{donor}$ offset. This general conclusion about our system stays valid even if we take into consideration uncertainties of energy levels in our system (see Fig. 1).

However, it is worth noticing that the fill factor of our experimental curve is lower than fill factors of the presented theoretical SQ curves, that should be ascribed to the existence of some parasitic resistances in the real system associated with non-radiative losses in the device. The shunt resistance calculated near *0* V equals *500* kΩ·cm² and may result from interface recombination. However, the value of series resistance cannot be characterized by a certain value because the current deviates from a direct voltage proportionality with increasing voltage.

Nevertheless, even though the obtained experimental $V_{oc}$ seems to be relatively high, the value of the short-circuit current is more than 4 times lower than the theoretical values predicted by the SQ limit for the same absorptivity, namely *0.86*, of an ideal semiconductor device and the excitonic cell. The fact that the experimental value of $J_{sc}$ is lower than these theoretical values may be attributed to the fact, that the thickness of the donor layer is several times larger than the respective exciton diffusion length reported for this layer [13,22]. Thus, despite the high absorptivity of the system, not all of excitons reach the active DBP/PTCBI interface within their lifetime, and so, not all of these excitons may contribute to the current flow. Hence, the photogenerated current can be expressed as follows:

$$J_G = e\, f\, a_o I_o \tag{5}$$

where *f* is the probability that an exciton generated in the cell dissociates at the donor/acceptor interface, equal to about *24*% in the case of our cell. If we put Eq. (5) at *f=24*% in Eqs. (2) and (3), then the SQ model leads to dashed-dotted line in Fig. 4. Short-circuit current values for experimental and theoretical results at *f=0.24* coincide with each other. However, near open-circuit voltage the experimental and theoretical curves diverge clearly. It is difficult to determine the causes of this phenomenon, but we suppose that it can be affected by space charge formed by charges separated at donor-acceptor interface. Enhancement of the performance of the cell

would require the increase in the value of f. Respecting Lambert-Beer law and the fact that only excitons generated within a certain distance from the active D/A interface equal to the exciton diffusion length in each of the active layers, we may use the following formula to estimate the flux of excitons $G_{ex}$ contributing to the photocurrent:

$$G_{ex} = \int_{d_1-L_{D1}}^{d_1+L_{D2}} \left(-\frac{dI}{dx}\right) dx = I_o e^{-\kappa_1 d_1}(e^{\kappa_1 L_{D1}} - 1) + I_o e^{-\kappa_1 d_1}(1 - e^{-\kappa_2 L_{D2}}) \quad (6)$$

where $I_0$ is the intensity of light incident on the ITO/$MoO_x$ interface, while $d_1$ stands for the thickness of the donor layer, $\kappa_1$ and $\kappa_2$ denote linear absorption coefficients of the donor and acceptor layers, while $L_{D1}$ and $L_{D2}$ are exciton diffusion lengths in these materials, respectively. This flux, calculated for the exciton diffusion lengths reported in literature, equal to *16* nm in the case of DBP [13] and *5* nm for PTCBI [17,38,39], divided by the incident photon flux of $10^{14}$ $cm^{-2}s^{-1}$ gives the estimated value of the probability, that an incident photon generates an exciton capable of dissociation. The value of this probability for the investigated cell is equal to *21*%. It correlates well with the external quantum efficiency of our device, equal to *20.75*%, and the estimated *24*% probability that an exciton generated in the cell dissociates at the donor/acceptor interface, suggesting that excitons reaching the active interface dissociate into free charge carriers very effectively. Moreover, the order of magnitude of $G_{ex}$ implies, that exciton diffusion length in the DBP layer in our system is consistent with the value reported by Xiao et al. [13], that is much larger than the values of this parameter suggested in literature by Yokoyama et al. [22] (see Table 2).

**Table 2.** Photovoltaic parameters of the real and modeled cells of the same absorptivity of *0.86* obtained under monochromatic illumination of $\lambda_o$=*615* nm and $I_o$=$10^{14}$ $cm^{-2}s^{-1}$.

| Type of a cell | $V_{oc}$ (mV) | $I_{SC}$ (μA/cm²) | FF | η (%) |
|---|---|---|---|---|
| Real, ITO/MoO3/DBP/PTCBI/BCP/Ag | 580 | 3.32 | 0.52 | 3.0 |
| Ideal semiconductor with $E_g$=1.0 eV | 545 | 13.80 | 0.85 | 19.1 |
| Ideal semiconductor with $E_g$=1.1 eV | 640 | 13.80 | 0.87 | 23.0 |
| Ideal excitonic cell with $E_g$=1.7 eV, $LUMO_{acceptor}$- $HOMO_{donor}$=1.0 eV, and *f*=1 | 715 | 13.80 | 0.88 | 26.0 |
| Ideal excitonic cell with $E_g$=1.7 eV, $LUMO_{acceptor}$ - $HOMO_{donor}$ =1.0 eV, and *f*=0.24 | 680 | 3.30 | 0.88 | 5.9 |

Moreover, $V_{oc}$ and $J_{sc}$ measured at illumination of $10^{14}$ $cm^{-2}s^{-1}$ practically do not change within the *520* nm-*620* nm spectral range, for which they reach the maximum values. The energy conversion efficiency under monochromatic illumination of intensity $I_0$=$10^{14}$ $cm^{-2}s^{-1}$, and wavelength $\lambda_o$=*615* nm equals *3*%. The illumination of $10^{14}$ $cm^{-2}s^{-1}$ at *615* nm corresponds to *97* lux, which is the range of typical value of illuminance on corridors. Therefore, we think that photovoltaic cells based on DBP/PTCBI junction could be consider for indoor applications.

**Conclusions**

The investigated system exhibits quite high value of open-circuit voltage, in comparison to the SQ limits calculated for ideal single-junction semiconductor devices of bandgaps close to the $LUMO_{PTCBI}$-$HOMO_{DBP}$ offset or crystalline silicon of the same absorptivity. Even though our device was not optimized it already shows a *3*% power conversion efficiency under low intensity of illumination at $\lambda$=*615* nm. Our research confirms that the DBP/PTCBI junction enables effective dissociation of excitons at donor-acceptor interface with efficient conversion of exciton energy to chemical energy of electron-hole pair. This conclusion is in a contradiction with the research performed on photovoltaic cell with DBP/PTCBI junction and presented in Ref. [28], where poor photovoltaic properties have been reported.

Moreover, $V_{oc}$ and $J_{sc}$ measured at illumination of $10^{14}$ $cm^{-2}s^{-1}$ practically do not change within the *520* nm-*620* nm spectral range, for which they reach the maximum values. Therefore, we think that photovoltaic cells based on DBP/PTCBI junction could be consider for indoor applications.

## References


[1] M.A. Green, H. Hishikawa, E.D. Dunlop, D.H. Levi, J. Hohl-Ebinger, A.W.Y. Ho-Baillie, Prog. Photovolt. Res. Appl. 26 (2018) 427.
[2] W. Shockley, H. Queisser, J. Appl. Phys. 32 (1961) 510.
[3] M. Freunek (Müller, M. Freunek, L.M. Reindl, IEEE J. Photovolt. 3 (2013) 59.
[4] B. Mimaert, P. Veelaert, Energies 7 (2014) 1500.
[5] P. Würfel, Physics of Solar Cells, WILEY-VCH Verlag GmbH&Co. KGaA, Weinheim, 2005.
[6] D. Guo, D. Brinkman, A.R. Shaik, C. Ringhofer, D. Vasileska, J. Phys. D Appl. Phys. 51 (2018) 153002.
[7] Z. Xie, S. Sun, Y. Yan, W. Wang, L. Qin, G.G. Qin, J. Phys. D Appl. Phys. 49 (2016) 275106.
[8] J.E.M. Haverkort, E.C. Garnett, E.P.A.M. Bakkers, Appl. Phys. Rev.- Focus. Rev. 5 (2018) 031106.
[9] T. Kirchartz, P. Kaienburg, D. Baran, J. Phys. Chem. C 122 (2018) 5829.
[10] Y. Peng, L. Zhang, T.L. Andrew, Appl. Phys. Lett. 105 (2014) 083304.
[11] A. Hassan, B. Kadem, W. Cranton, Thin Solid Films 636 (2017) 760.
[12] H. Liang, Z. Luo, R. Zhu, Y. Dong, J.-H. Lee, J. Zhou, S.-T. Wu, J. Phys. D Appl. Phys. 49 (2016) 145103.
[13] X. Xiao, J.D. Zimmerman, B.E. Lassiter, K.J. Bergemann, S.R. Forrest, Appl. Phys. Lett. 102 (2013) 073302.
[14] M. Zhang, H. Wang, H. Tian, Y. Geng, C.W. Tang, Adv. Mater. 23 (2011) 4960.
[15] S. Nam, J. Seo, M. Song, H. Kim, M. Ree, Y.-S. Gal, D.D.C. Bradley, Y. Kim, Org. Electron. 48 (2017) 61.
[16] I.G. Hill, J. Schwartz, A. Kahn, Org. Electron. 1 (2000) 5.
[17] P. Peumans, A. Yakimov, A. Forrest, J. Appl. Phys. 93 (2003) 3693.
[18] H.B. Michaelson, J. Appl. Phys. 48 (1977) 4729.
[19] C.W. Tang, Appl. Phys. Lett. 48 (1986) 183.
[20] T. Zhuang, T. Sano, J. Kido, Org. Electron. 26 (2015) 415.
[21] D. Fujishima, H. Kanno, T. Kinoshita, E. Maruyama, M. Tanaka, M. Shirakawa, K. Shibata, Sol. Energy Mater. Sol. Cells 93 (2009) 1029.
[22] D. Yokoyama, Z.Q. Wang, Y.-J. Pu, K. Kobayashi, J. Kido, Z. Hong, Sol. Energy Mater. Sol. Cells 98 (2012) 472.
[23] M.C. Barr, C. Carbonare, R. Po, V. Bulović, K.K. Gleason, Appl. Phys. Lett. 100 (2012) 183301.
[24] K. Liu, T.T. Larsen-Olsen, Y. Lin, M. Beliatis, E. Bundgaard, M. Jorgensen, F.C. Krebs, X. Zhan, J. Mater. Chem. 4 (2016) 1004.
[25] C.T. Howells, S. Saylan, H. Kim, K. Marbou, T. Aoyama, A. Nakao, M. Uchiyama, I.D.W. Samuel, D.-W. Kim, M.S. Dahlem, P. Andre, J. Mater. Chem. 6 (2018) 16012.
[26] K.H. Park, Y. An, S. Jung, H. Park, C. Yang, Energy Environ. Sci. 9 (2016) 3464.
[27] C.B. Nielsen, S. Holliday, H.-Y. Chen, S.J. Cryer, I. McCulloch, Accounts Chem. Res. 48 (2015) 2803.
[28] K.C. Song, R. Singh, J. Lee, D.H. Sin, H. Lee, K. Cho, J. Mater. Chem. C 4 (2016) 10610.
[29] K.J. Lee, J.H. Woo, Y. Xiao, E. Kim, L.M. Mazur, D. Kreher, A.-J. Attias, K. Matczyszyn, M. Samoc, B. Heinrich, S. Méry, F. Fages, L. Mager, A. D'Aléo, J.W. Wu, F. Mathevet, P. André, J.-C. Ribierre, RSC Adv. 6 (2016) 57811.
[30] A. Adamow, L. Sznitko, E. Chrzumnicka, J. Stachera, A. Szukalski, T. Martynski, J. Myśliwiec, Sci. Rep. 9 (2019) 2143.
[31] J. Sworakowski, J. Lipiński, K. Janus, Org. Electron. 33 (2016) 300.
[32] Y.-Q. Zheng, W.J. Potscavage Jr., T. Komino, M. Hirade, J. Adachi, C. Adachi, Appl. Phys. Lett. 102 (2013) 143304.
[33] J. Szostak, R. Signerski, J. Godlewski, Phys. Status Solidi A 210 (2013) 2353.
[34] R. Marczyński, J. Szostak, R. Signerski, G. Jarosz, Synth. Met. 245 (2018) 245.
[35] H. Lee, S.W. Cho, Y. Yi, Curr. Appl. Phys. 16 (2016) 1533.
[36] S. Sachdeva, J. Kaur, K. Sharma, S.K. Tripathi, Curr. Appl. Phys. 18 (2018) 1592.
[37] M.B. Upama, M. Wright, N.K. Elumalai, M.A. Mahmud, D. Wang, K.H. Chan, C. Xu, F. Haque, A. Uddin, Curr. Appl. Phys. 17 (2017) 298.
[38] O.V. Mikhnenko, P.W.M. Blom, T.-Q. Nguyen, Energy Environ. Sci. 8 (2015) 1867.
[39] S.-B. Rim, R.F. Fink, J.C. Schöneboom, P. Erk, P. Peumans, Appl. Phys. Lett. 91 (2007) 173504.
[40] Y. Wang, R. Ding, F. Huang, D. Ma, Synth. Met. 244 (2018) 61.
[41] H. Kumar, P. Kumar, N. Chaudhary, R. Bhardwaj, S. Chand, S.C. Jain, V. Kumar, J. Phys. D Appl. Phys. 42 (2009) 015102.
[42] L. Nian, Y. Kan, H. Wang, K. Gao, B. Xu, Q. Rong, R. Wang, J. Wang, F. Liu, J. Chen, G. Zhou, T.P. Russell, A.K.-Y. Jen, Energy Environ. Sci. 11 (2018) 3392.
[43] W. Zhao, D. Qian, S. Zhang, S. Li, O. Inganäs, F. Gao, J. Hou, Adv. Mater. 28 (2016) 4734.
[44] R. Janssen, J. Nelson, Adv. Mater. 25 (2013) 1847.
[45] S.M. Menke, N.A. Ran, G.C. Bazan, R.H. Fried, Joule 2 (2017) 25.
[46] N.C. Giebink, G.P. Wiederrecht, M.R. Wasilewski, S.R. Forrest, Phys. Rev. B 83 (2011) 195326.
[47] K. Seki, A. Furube, Y. Yoshida, Jpn. J. Appl. Phys. 54 (2015) 08KF04.